1 Introduction

1.1 Delaunay triangulation

There are several models of spatial networks. Many of them are described in the review [1]. In another recent review [2], Barthélemy explores different kind of transitions in spatial networks.

The Delaunay triangulation (DT) is the dual of the Voronoi-Tessellation. Given a set of points V in a d-dimentional space, a link between two nodes $u,\ v \in V$ is present if and only if there exist a d-dimentional sphere which embeds u and v but no other points. Several properties of the DT have been studied, such as extreme values [3], average degree and distance [CITE], ... [AGREGAR MAS COSAS]. Although a naive algorithm for constructing a Delaunay triangulation is $\mathcal{O}(N^3)$, the complexity can be reduced to $\mathcal{O}(N \log N)$, as shown in [3]. In this work, we used the Qhull computational geometrical library [1], together with the Python SciPy package.

The percolation properties of DT have been studied in [4, 5].

1.2 Betweenness centrality

There are multiple metrics to adress node centrality. In a recent work, many among the most popular ones were compared, and the correlation between them in different kind of networks was studied [6].

Betweenness centrality (BC) was independently proposed by [7] and [CITE]. The computational complexity of the BC is $\mathcal{O}(NM)$ [8].

Different variations to the original Brandes algorithm are discussed in [9], including k-betweenness.

In [10, 11], Ercsey-Ravasz, et al. study the so-called k-betweenness centrallity, which is similar to betweenness centrality but where only paths no longer than k are considered. The authors show that the k-betweenness distributions present a scaling, where the curves corresponding to different values of k can be scaled into a universal curve. In addition, they argue that a moderate value of k is sufficient for identifying the influencer nodes.

In [12], Kirkley, et al. show that the road networks of the largest cities of the world have a universal betweenness distribution. This distribution appears as the result of two main contributions. The minimum spannig tree, which gives a power-law distribution $p(b) \sim b^{-1}$ in the range (N, N^2), and the shorcuts, which allow nodes with lower betweenness (in the range $(1, N)$).

In spatial networks, it is interesting to study the spatial distribution of high betweenness nodes. Using a model based on real data from road networks and Delaunay triangulations, in [12] the authors show that there exist a transition in the spatial distriution of these nodes. For a sparse network, the nodes are distributed rather inhomogeneously and relatively further from the center. As the network becomes denser, the distribution moves toward the center and becomes more homogenous.

In road networks, sometimes there are large loops composed by nodes of very high betweenness [13].

1.3 Percolation transition

Percolation transition on random spatial networks has been largely studied [14, 4, 15]. Although the location of the percolation threshold depends on the model studied, in general the universaillity class is the same as regular lattices. In particular, Norrenbrock, et al [16] study the percolation transiton for recalculated degree-based (RD) and betweenness-based (RB) attacks on four different models of spatial networks. They conclude that the RD attack belongs to the standard 2-d percolation transition universality class. With respect to RB, they show that the percolation threshold is located at $f_c = 0$, but they do not arrive at a conclusion regarding other characteristics of the transition.

For 2-dimensional regular lattices, the exponents are

[1] www.qhull.org

$$\beta = 5/36 \simeq 0.14, \tag{1}$$
$$\gamma = 43/18 \simeq 2.39, \tag{2}$$
$$\tau = 187/91 \simeq 2.05, \tag{3}$$
$$\nu = 4/3. \tag{4}$$

Exponentes en 2D

$$\frac{\gamma}{2\nu} = 0.896 \tag{5}$$
$$1 - \frac{\beta}{2\nu} = 0.948 \tag{6}$$

For a finite-size system, the percolation threshold does not necesarly coincide with the corresponding value for $N \to \infty$. In general, the difference between these values presents a scaling in the form

$$f_c(N) - f_c = bN^{-1/\theta}. \tag{7}$$

TODO: Chequear cuál es el exponente correcto en la ecuación anterior. Partiendo del scaling

$$X_1 \sim N^{-\omega/(d\nu)} F[(f - f_c)N^{1/(d\nu)}], \tag{8}$$

donde $\xi = |f - f_c|^{-\nu}$, y definiendo $f_c(N) = \max_f \left\{F[(f - f_c)N^{1/(d\nu)}]\right\}$, tenemos que F alcanza su máximo para un valor b tal que $b = (f_c(N) - f_c)N^{1/(d\nu)}$, de donde se deduce que $\theta = 1/(d\nu)$ (ver [17, 18]). Sin embargo, hay otros trabajos que dicen que esto no siempre es así, por ejemplo, en [19] dicen que $\theta = \nu_1$ y que, en general, $\nu_1 \neq \nu$ (en algunos casos, como por ejemplo en percolación random, sí coinciden). En [20], dicen que $\theta = d_u/2$, siendo d_u la dimensión crítica superior.

In a recently published article, Fan, et al. proposed a new method to analyze generalized percolation processes, based on the scaling of the largest jump in the order parameter during the process [19]. Although the authors deal with bond percolation, the same analysis can be performed for site percolation. Based on this work, we define

$$\Delta = \frac{1}{N} \max_t \left[N_1(t+1) - N_1(t)\right], \tag{9}$$

where $N_1(t)$ is the size of the largest cluster after t nodes are removed from the network. According to [19], $\Delta \sim L^{-\beta/\nu}$. We also define t_c as the number of nodes removed such that the maximum in 9 is attained. In the thermodynamic limit, the percolation threshold coincides with $r_c = t_c/N$. Finally, the percolation strength is defined as $N_1(t_c)$. According to [19], these quantities, averaged over realizations, scale as

$$\Delta \sim L^{-\beta/\nu} \tag{10}$$
$$r_c(L) - r_c(\infty) \sim L^{-1/\nu_1} \tag{11}$$
$$N_1(L) \sim L^{-d_f}. \tag{12}$$

Also, the fluctuations for these quantities present a similar scaling

$$\chi_\Delta \sim L^{-\beta/\nu} \tag{13}$$
$$\chi_{r_c} \sim L^{-1/\nu} \tag{14}$$
$$\chi_{N_1} \sim L^{-d_f}. \tag{15}$$

Note that exponent ν_1 does not coincide in general with the correlation length critical exponent ν.

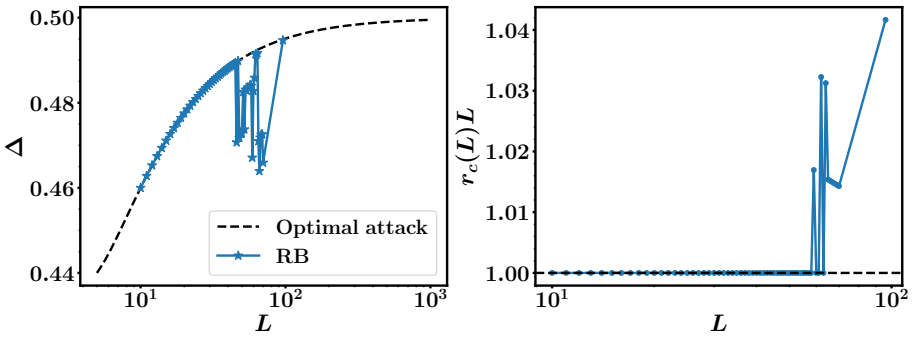

Figure 1: (Left) Maximum jump in the order parameter in a single realization of the RB attack over a 2-d lattice. Black curve: $\Delta = \frac{1}{2} - \frac{1}{2L} + \frac{1}{L^2}$, corresponding to split the lattice in halves. (Right) Scaling of the critical point for finite-size systems. As it can be seen, the RB attack performs almost optimally in this netowork

1.3.1 Percolation transition with $f_c = 0$

References describing processes where $f_c = 0$: [21, 22, 23]

Other useful references: [24, 22, 25]

2 Results

2.1 Characterization of the percolation transition

In Figure 3 we show the scaling of the gap exponents (Eqs. 10-15). The exponent corresponding to Δ —the largest relative jump in the largest cluster— is consistent with $\beta = 0$ including uncertainty, which gives a strong evidence of a first-order transition. At first sight, it brings attention that $\Delta(L)$ increases with L, but this can be explained by finite-size effects (see Section 2.2). In addition, we can see that the largest cluster is not a fractal, as its scaling is consistent with $d_f = 2$, also consistent with a discontinuous transition. Regarding the percolation threshold, we can see from panel (c) that $r_c = 0$ gives a good power-law , thus indicating that the transition occurs at the origin of the process in the thermodynamic limit, in accordance with [16].

2.2 Optimal attack on Lattices

For a d-dimensional lattice, the optimal attack consists in breaking the network by recursively removing the nodes located over a d-1 hyperplane which intersects the center of the giant component. The largest jump in the giant component is then given by

$$\Delta = \frac{1}{L^d}\left[L^d - L^{d-1} + 1 - L^{d-1}\frac{L-1}{2}\right] = \frac{1}{2} - \frac{1}{2L} + \frac{1}{L^d}, \tag{16}$$

and the position of the largest jump is located at $r_c = L^{-1}$. Although the largest relative jump goes to $1/2$ as $L \to \infty$, the value for finite-size systems is lower. The RB attack performs almost optimally for the 2D Lattice, as it can be seen in 1.

2.3 Breaking nodes and fractals

In Figure 2 we show the network status after the first t_c nodes are removed (i.e., right after the largest relative jump of the giant cluster takes place). We compare the 2D Lattice (left panels) with the DT (right panels), and different attacks. As the figure shows, the RB attack cuts the lattice by the main diagonal, and breaks the DT in two extensive components. Thus, we call this set of nodes the *breaking nodes*.

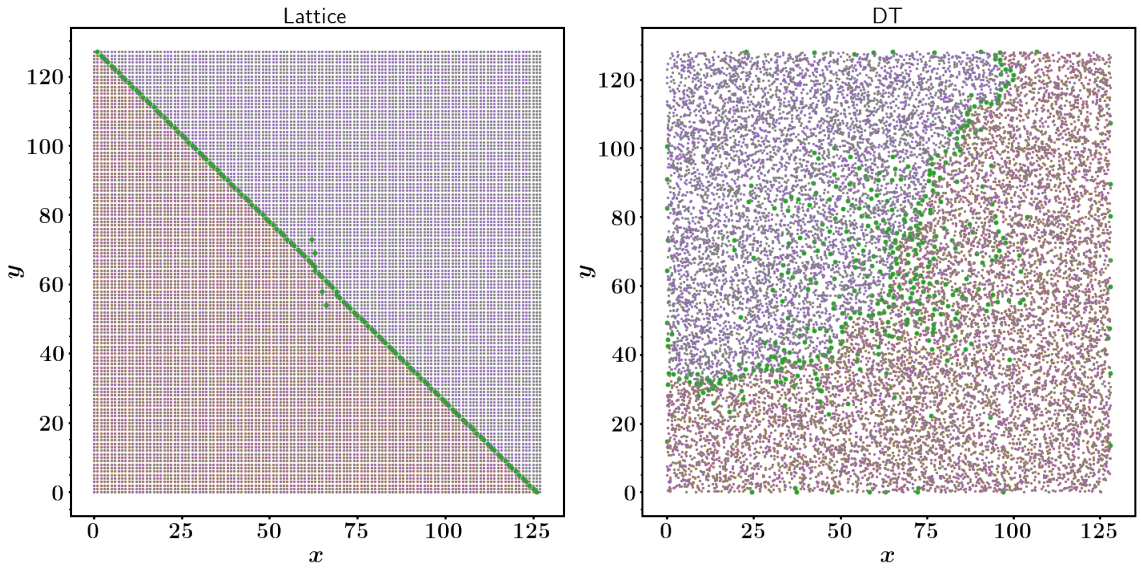

Figure 2: Network status at f_c for RB ($N = 128^2$). After removing the green nodes, the network is splitted in two extensive clusters. The largest cluster correspond to the orange nodes and the second largest cluster to the purple nodes. The rest of the nodes are plotted in grey. For the Lattice, RB traces a diagonal and break the network in two clusters of almost the same size. For DT, the algorithm starts by removing the high-betweennesss nodes located at the periphery and then it finds a high betweenness "percolating path" across the network. Although in the latter case the network is also splitted in two extensive components, there is a significant difference in size between the two largest clusters.

To characterize the geometry of the *breaking nodes*, we estimated its fractal dimension using two common methods [CITE: Stanley book]. The first method, known as the box-counting method, consists in covering the space by non-overlapping boxes of linear size $\delta \leq L$ and count the number N_B of such boxes containing at least one node belonging to the set. The procedure is repeated for different values of δ. Fractal objects are expected to follow a relation $N_B(\delta) \sim \delta^{-d_B}$, where d_B, known as the box-counting dimension, is its characteristic length. For the second method, we select a random element of the set and consider a square window of linear size l centered at the element. We count the number of elements of the set in the window and repeat the procedure for different values of l. We then average these values taking several seeds. For each value of l, the mass $M(l)$ is computed as the average over seed elements of the number of nodes in the window, and is expected to follow the scaling $M(l) \sim l^{d_f}$, where d_f is the fractal dimension of the set. In Figure 1 we show both estimations for the DT network and for the 2D Lattice. Coincident with Figure 2, the fractal dimension for the set of removed nodes from the Lattice is equal to one, as the nodes are roughly arranged over a straight line. For the case of DT, a non-trivial scaling is seen, with a fractal dimension greater than one. Note that the values obtained using both methods are consistent ($d_B = 1.45 \pm 0.16$ and $d_f = 1.43 \pm 0.06$).

There is a third way of estimating the fractal dimension of the set, which consists in using Equation 11. According to this equation, the mass of the set scales as $M \sim N^{1-1/\nu_1} = L^{d_{f_2}}$, where $d_{f_2} := 2(1-1/\nu_1)$. Taking the value estimated for ν_1, one obtains $d_{f_2} = 1.44$.

The breaking nodes for the case of RB on the Lattice consist mainly in one of the main diagonals. Thus, if we take the spanning subgraph with vertex set equal to the breaking nodes, we have mainly isolated nodes. In contrast, when applying the same attack to the DT, the spanning subgraph corresponding to the breaking nodes has a large connected component. We call this component the *backbone* of the breaking nodes. In Figure 5, we measure the fractal dimension of this set. We can see that, in this case, the fractal dimension of the set is close to one, indicating that the backbone is not fractal, but a conventional curve.

As it can be infered from Figure 2, the backbone itself is sufficient to break the network. We corroborated this proposition by measuring the relative size of the largest cluster after removing only the backbone nodes. As Figure **??** shows, S_1 has a comparable size after removing the backbone with the result of removing all the breaking nodes. In terms of attack performance, we can say that, although the RB attack is very efficient in breaking the network (the percolation threshold is $r_c = 0$ in the thermodynamic limit), is not optimal, as the number of nodes that the attack removes scales more that linearly. But, if instead of removing the breaking nodes, they are only algorithmically identified, one can chose to remove only the backbone, disconnecting the network with an efficiency now close to

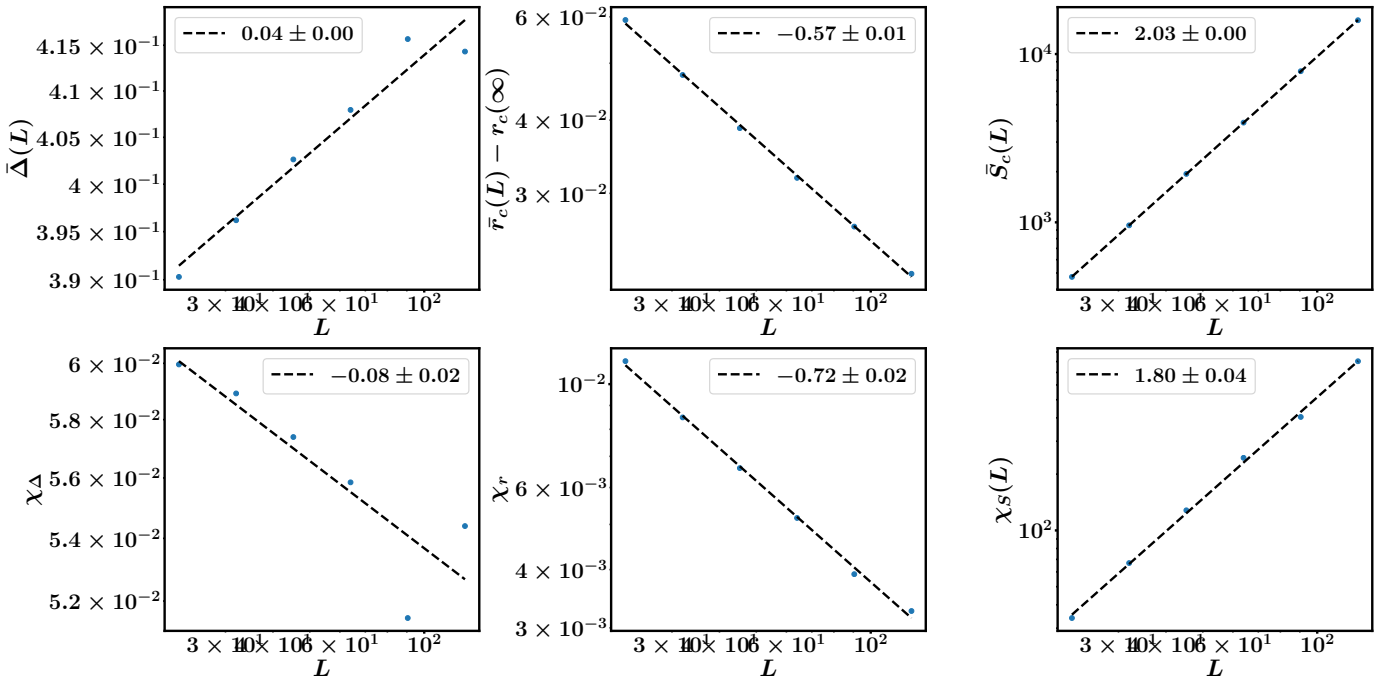

Figure 3: Estimation of the critical exponents using the gap scaling proposed by Fan, et al. in [19], and taking $r_c(\infty) = 0$.

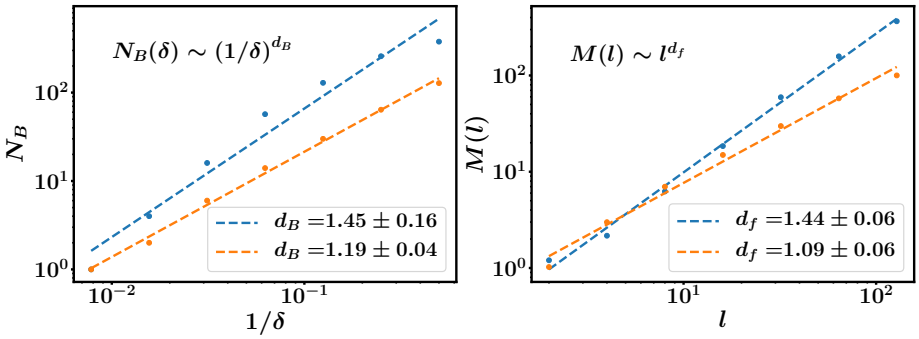

Figure 4: Fractal dimension of the breaking nodes for networks of size $N = 128^2$. Left: Box-counting dimension; Right: estimation based on random seed sampling. (Blue) DT; (Orange) 2D Lattice.

optimal.

2.4 Attacks with approximate betweenness

In this section we compare the RB attack with attacks using ℓ-betweenness, i.e, computing betweenness using only paths up to length ℓ.

References

[1] Marc Barthélemy. Spatial networks. *Physics Reports*, 499(1-3):1–101, 2011.

[2] Marc Barthelemy. Transitions in spatial networks. *Comptes Rendus Physique*, 19(4):205–232, 2018.

[3] D. T. Lee and B. J. Schachter. Two algorithms for constructing a Delaunay triangulation. *International Journal of Computer & Information Sciences*, 9(3):219–242, 1980.

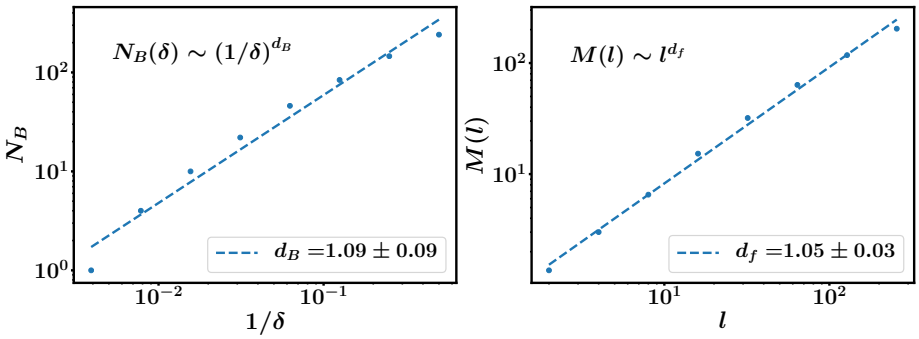

Figure 5: Fractal dimension of the backbone for a network of type DT of size $N = 256^2$. Left: Box-counting dimension; Right: estimation based on random seed sampling.

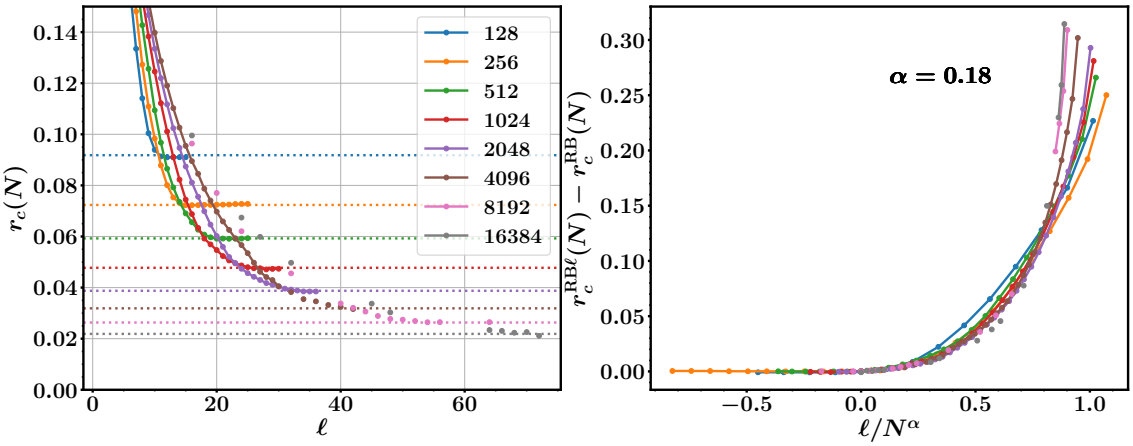

Figure 6: (Left) Shift of the position of the percolation threshold for the RB attacks with cutoffs. Dashed lines indicate the corresponding valu for the RB attack. (Right) Scaling of the ℓ^* with the system linear size. Here, ℓ^* is defined as the minimum ℓ such that the percolation threshold for the RB-ℓ^* differs from the full RB attack in less than 1%.

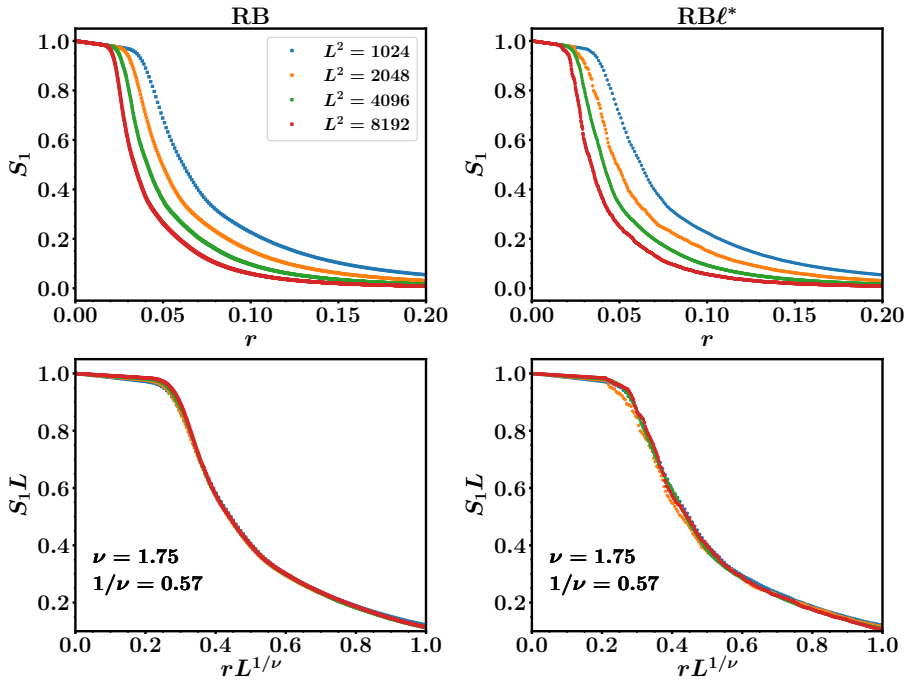

Figure 7: (Left) Collapse for the order parameter S_1 for networks attacked using the RB strategy. (Right) The same, but using RBℓ^*, where the value of ℓ^* was obtained in the same way as for Figure 6.

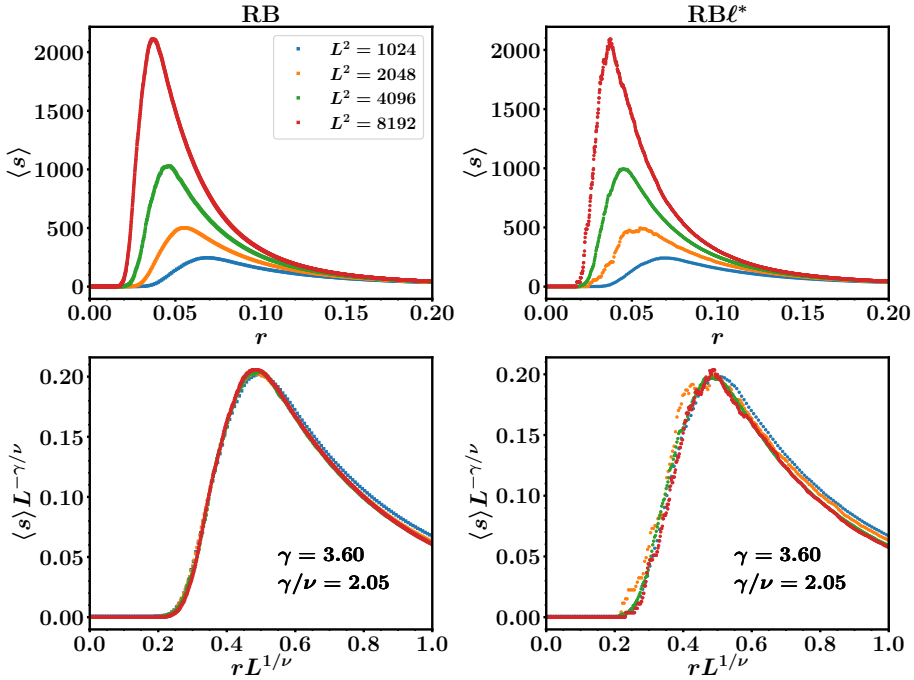

Figure 8: (Left) Collapse for the susceptibility $\langle s \rangle$ for networks attacked using the RB strategy. (Right) The same, but using RBℓ^*, where the value of ℓ^* was obtained in the same way as for Figure 6.

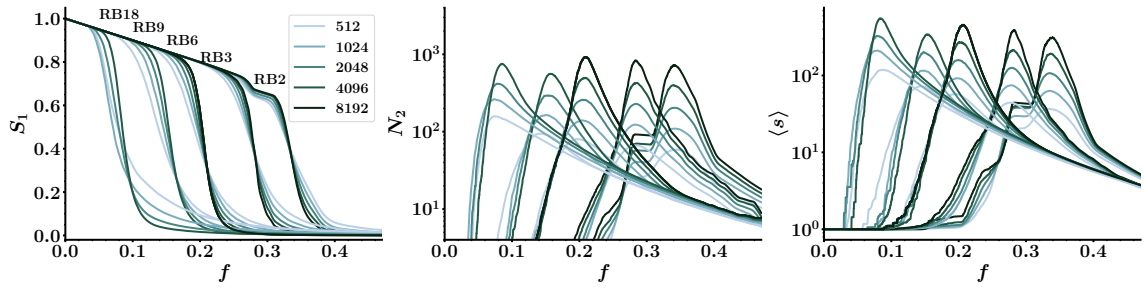

Figure 9: Oder parameter, susceptibility and size of second lurgest cluster for RB and RB with different cutoffs, for different sizes. Note that for the RB attack, the peak in the susceptibility and second largest cluster tends to shift to lower values of f. Instead, for approximate attacks the shift is not clear.

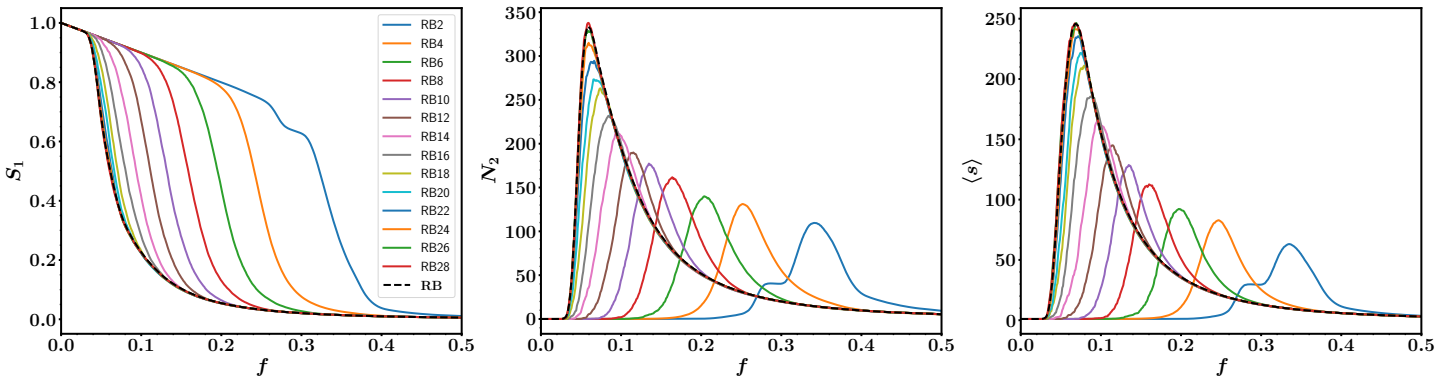

Figure 10: Oder parameter, susceptibility and size of second lurgest cluster for RB and RB with different cutoffs. $N = 1024$. As larger path lengths are taken into account, the attack becomes more efficient in dismantling the network, and the transition moves towards lower values of f. Also the peak in the susceptibility and second largest cluster increases, showing that the fluctuations become more relevant. Except for RB2, all curves corresponding to attacks with cutoff present a similar form. The case of RB2 deserves special attention, as it presents a sort of double transition.

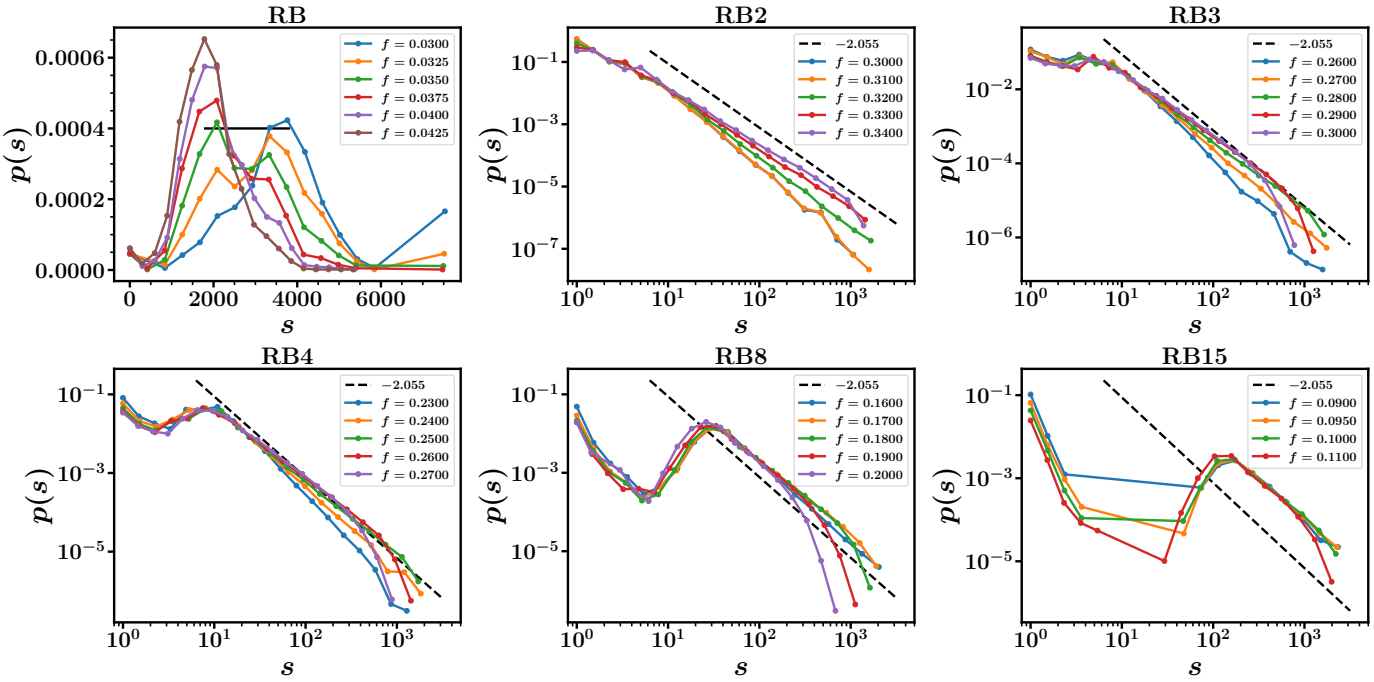

Figure 11: Finite component size distribution near the percolation threshold for RB and RB with different cutoffs. For RB, the giant cluster is also considered. Each histogram is generated over an average of $N_r = 1000$ network realizations. The dashed line corresponds to $p(s) \sim s^{-\tau}$, with $\tau = 0.2055$, which is the correspondig value for random percolation. The attack based on the simpler approximation of BC (taking only paths of length 2), shows a power-law distribution consistent with standard percolation. As longer lengths are added to the approximation, the distribution starts to deviate from the power-law, presenting a valley for lower cluster sizes. For RB, the power-law dependence is not seen at all. Instead, a narrow-tailed bimodal distribution is seen, which is consistent with a first order transition [26, **?**] . The difference between the peaks is roughly the value for the largest jump in the giant component, $\Delta \sim 0.4$.

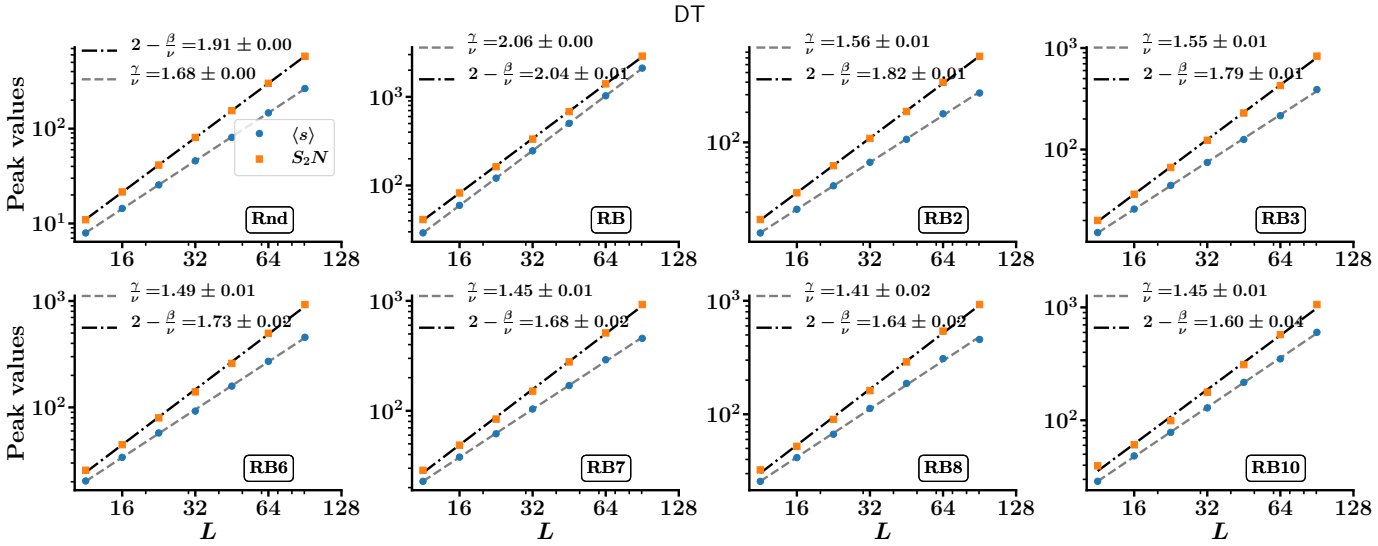

Figure 12: Scaling for the peak in the susceptibility and second largest cluster for RB and RB with different cutoffs. For standard percolation in 2-dimensional regular lattices, the corresponding values are $\frac{\gamma}{2\nu} = 0.896$ and $1 - \frac{\beta}{2\nu} = 0.948$. For RB, the scaling is consistent with a first-order transition, where $\beta = 0$ and $\gamma/(d\nu) = 1$ [27, 28, 18].

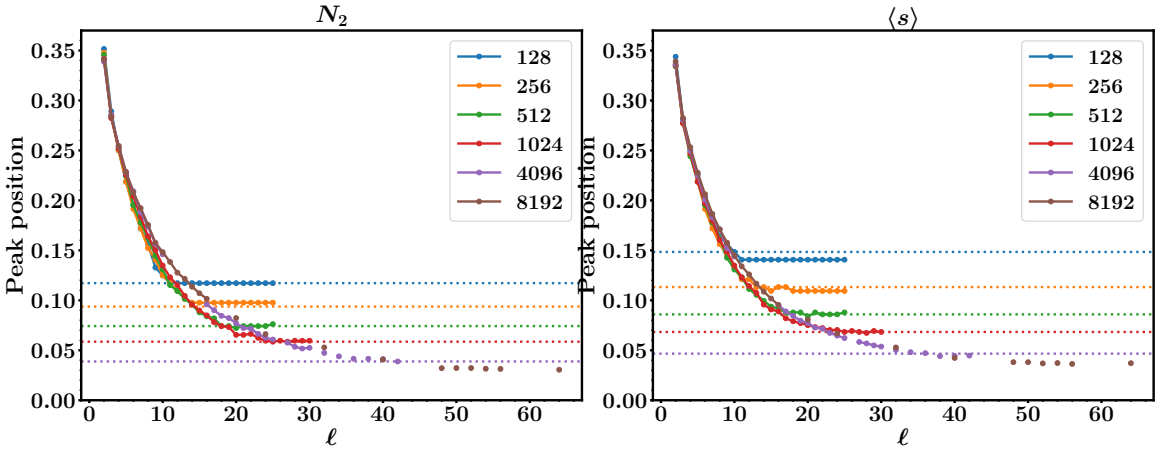

Figure 13: (Upper panels) Shift of the position of the susceptibility and second largest cluster peak for the RB attacks with cutoffs. Dashed lines correspond to the position of the peak for the RB attack. (Lower panels) Difference between the peak for RB attack with cutoff and RB. The x axis is scaled by the average initial diameter D of the networks for each size.

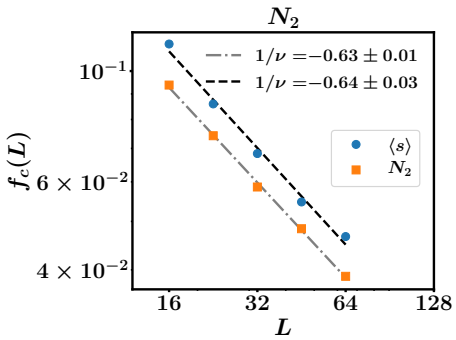

Figure 14: Position of the peak in the susceptibility and second largest cluster as a function of the inverse network size, for the RB attack. The data is consistent with a scaling of the form of Eq. 7, with $f_c = 0$ and $\theta \simeq 3$. This implies that, for the thermodynamic limit $N \to \infty$, only a sub-linear fraction of nodes has to be removed in order to dismantle the network. This result is consistent with the result obtained by [16], using a scaling for the area under the curve of the order parameter.

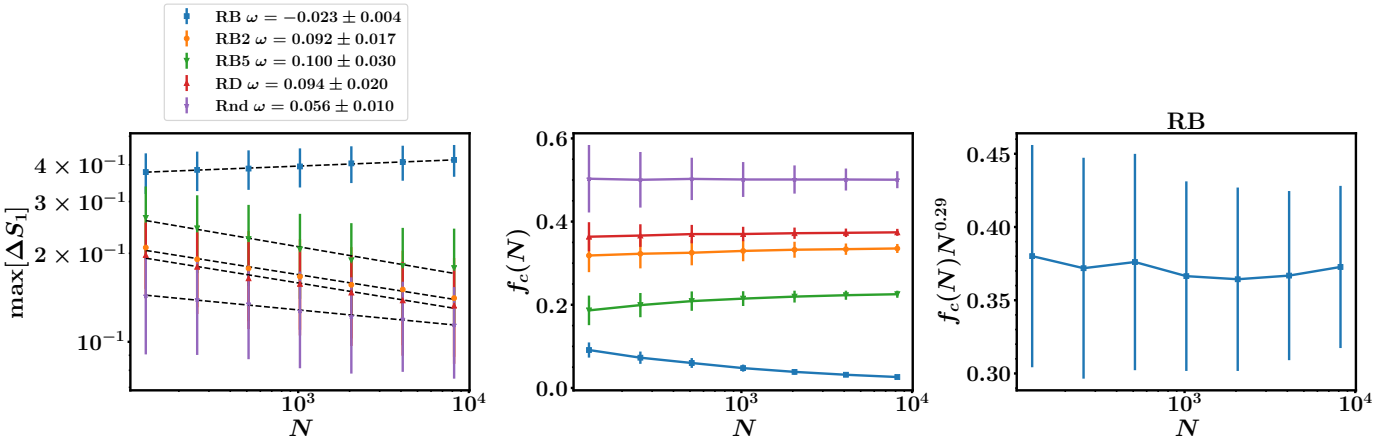

Figure 15: (Left) Average for the maximum variation in the order parameter for different attacks. Dashed lines correspond to a power-law fit $\Delta := \max[\Delta S_1] \sim N^{-\omega}$. The value for ω should be lower than zero for second-order transitions, and equal to zero for first-order transitions. References: [22, 29, 30, 19]. (Center) Finite-size percolation threshold, compued as the fraction of nodes correspondig to the largest jump in the order parameter. Except for RB, $f_c(N)$ quickly converges to a non-zero value. RB, in turn, converges to zero. (Right) Scaling of $f_c(N)$ for RB. The fact that, for local rules as RB with cutoff, the percolation threhold is non-zero, but for global rules, as RB, it goes to zero, resembles some explosive percolation models, such as the Spanning Cluster-Avoiding (SCA) method introduced in [31].

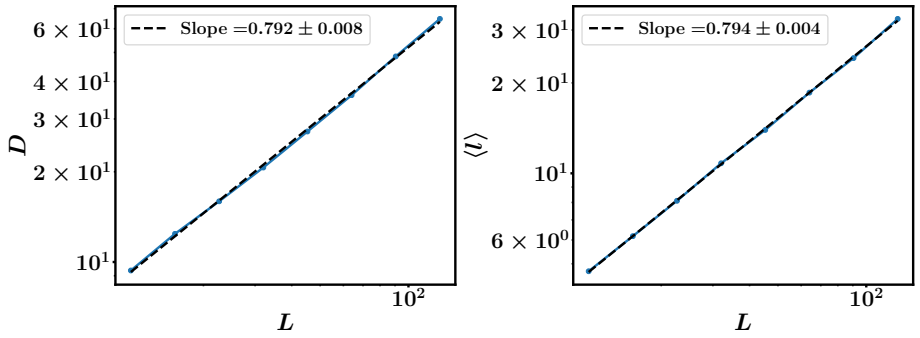

Figure 16: Diameter fo the DT as a function of the network size.

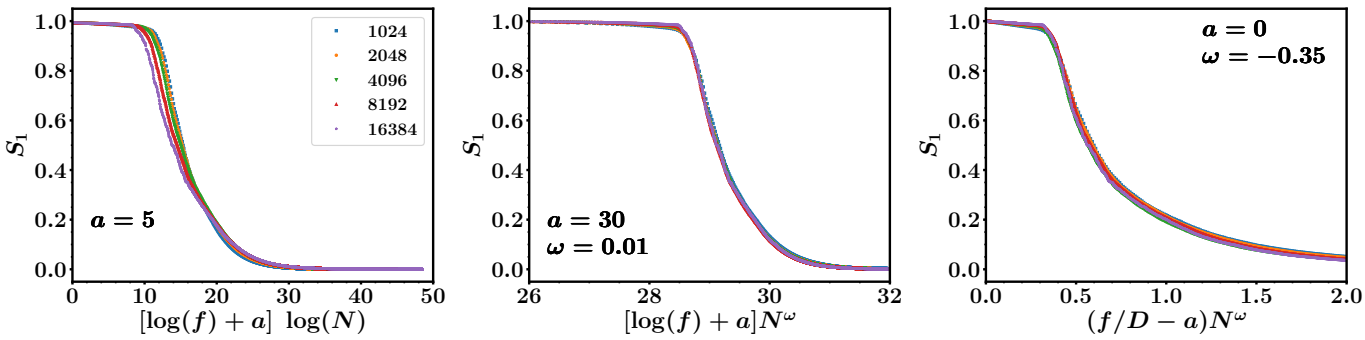

Figure 17: Different attempts to collapsing the curves correspondig to S_1 for different network sizes.

[4] Adam M. Becker and Robert M. Ziff. Percolation thresholds on two-dimensional Voronoi networks and Delaunay triangulations. *Physical Review E - Statistical, Nonlinear, and Soft Matter Physics*, 80(4):1–9, 2009.

[5] D. S.M. Alencar, T. F.A. Alves, G. A. Alves, A. Macedo-Filho, and R. S. Ferreira. Epidemic outbreaks on random Voronoi–Delaunay triangulations. *Physica A: Statistical Mechanics and its Applications*, 541:122800, 2020.

[6] Stuart Oldham, Ben Fulcher, Linden Parkes, Aurina Arnatkeviciūtė, Chao Suo, and Alex Fornito. Consistency and differences between centrality measures across distinct classes of networks. *PLoS ONE*, 14(7):1–23, 2019.

[7] Linton C Freeman. A Set of Measures of Centrality Based on Betweenness. *Sociometry*, 40(1):35, 1977.

[8] Ulrik Brandes. A faster algorithm for betweenness centrality*. *The Journal of Mathematical Sociology*, 25(2):163–177, 2001.

[9] Ulrik Brandes. On variants of shortest-path betweenness centrality and their generic computation. *Social Networks*, 30(2):136–145, 2008.

[10] Mária Ercsey-Ravasz and Zoltán Toroczkai. Centrality scaling in large networks. *Physical Review Letters*, 105(3):2–5, 2010.

[11] Mária Ercsey-Ravasz, Ryan N. Lichtenwalter, Nitesh V. Chawla, and Zoltán Toroczkai. Range-limited centrality measures in complex networks. *Physical Review E - Statistical, Nonlinear, and Soft Matter Physics*, 85(6), 2012.

[12] A Kirkley, H Barbosa, M Barthelemy, and G Ghoshal. From the betweenness centrality in street networks to structural invariants in random planar graphs. *Nature Communications*, 9(2018):2501, 2018.

[13] Benjamin Lion and Marc Barthelemy. Central loops in random planar graphs. *Physical Review E*, 95(4):1–12, 2017.

[14] O. Melchert. Percolation thresholds on planar Euclidean relative-neighborhood graphs. *Physical Review E - Statistical, Nonlinear, and Soft Matter Physics*, 87(4):1–7, 2013.

[15] Christoph Norrenbrock. Percolation threshold on planar Euclidean Gabriel graphs. *European Physical Journal B*, 89(5), 2016.

[16] C Norrenbrock, O Melchert, and A K Hartmann. Fragmentation properties of two-dimensional proximity graphs considering random failures and targeted attacks. *Physical Review E*, 94(6):1–11, 2016.

[17] Robert M Ziff. Scaling behavior of explosive percolation on the square lattice. *Physical Review E - Statistical, Nonlinear, and Soft Matter Physics*, 82(5):1–8, 2010.

[18] Y. S. Cho, J. S. Kim, J. Park, B. Kahng, and D. Kim. Percolation transitions in scale-free networks under the achlioptas process. *Physical Review Letters*, 103(13):1–4, 2009.

[19] Jingfang Fan, Jun Meng, Yang Liu, Abbas Ali Saberi, Jürgen Kurths, and Jan Nagler. Universal gap scaling in percolation SM. *Nature Physics*, 2020.

[20] R. A. Da Costa, S. N. Dorogovtsev, A. V. Goltsev, and J. F F Mendes. Explosive percolation transition is actually continuous. *Physical Review Letters*, 105(25):2–5, 2010.

[21] Hernán D Rozenfeld, Chaoming Song, and Hernán A Makse. Small-world to fractal transition in complex networks: A renormalization group approach. *Physical Review Letters*, 104(2):1–4, 2010.

[22] Alexander J Trevelyan, Georgios Tsekenis, and Eric I Corwin. Degree product rule tempers explosive percolation in the absence of global information. *Physical Review E*, 97(2):31–35, 2018.

[23] Y S Cho, S Hwang, H J Herrmann, and B Kahng. Avoiding a Spanning Cluster in Percolation Models. *Science*, 339(6124):1185–1187, 2013.

[24] Stefan Boettcher, Vijay Singh, and Robert M. Ziff. Ordinary percolation with discontinuous transitions. *Nature Communications*, 3, 2012.

[25] Y. S. Cho, S. W. Kim, J. D. Noh, B. Kahng, and D. Kim. Finite-size scaling theory for explosive percolation transitions. *Physical Review E - Statistical, Nonlinear, and Soft Matter Physics*, 82(4):2–5, 2010.

[26] N. A.M. Araújo and H. J. Herrmann. Explosive percolation via control of the largest cluster. *Physical Review Letters*, 105(3):2–5, 2010.

[27] K. Binder. Finite size scaling analysis of ising model block distribution functions. *Zeitschrift für Physik B Condensed Matter*, 43(2):119–140, 1981.

[28] K. Binder and D. P. Landau. Finite-size scaling at first-order phase transitions. *Physical Review B*, 30(3):1477–1485, aug 1984.

[29] N. Bastas, P. Giazitzidis, M. Maragakis, and K. Kosmidis. Explosive percolation: Unusual transitions of a simple model. *Physica A: Statistical Mechanics and its Applications*, 407:54–65, 2014.

[30] Jan Nagler, Anna Levina, and Marc Timme. Impact of single links in competitive percolation SM. *Nature Physics*, 7(3):265–270, 2011.

[31] Y. S. Cho, S. Hwang, H. J. Herrmann, and B. Kahng. Avoiding a Spanning Cluster in Percolation Models. *Science*, 339(6124):1185–1187, 2013.